Sliding Modes based Nonlinear PID Controller for Quadrotor: Theory and Experiment

Yasser Bouzid, Houria Siguerdidjane, Yasmina Bestaoui

Sliding Modes based Nonlinear PID Controller for Quadrotor
Theory and Experiment

Yasser Bouzid[1], Houria Siguerdidjane[2] and Yasmina Bestaoui[1]
[1]*IBISC Laboratoire, Université Paris-Saclay, Evry, France*
[2]*L2S, Centrale Supélec, Université Paris-Saclay, Gif sur yvette, France*

Keywords: UAV, Trajectory Tracking, Flight Control, Nonlinear PID.

Abstract: In this paper, a Nonlinear PID (NLPID) control design is proposed. The main idea consists of combining the classical sliding modes approach together with the PID structure. Unlike the existing nonlinear PID controllers in the literature, the coefficients are constant parameters in this work. Within this paper, we investigate the efficiency and the performance of this technique through an application to a small Vertical Take Off and Landing (VTOL) Unmanned Aerial Vehicle (UAV). The NLPID based autopilot drives the vehicle toward the desired configuration in the space while stabilizing the roll and the pitch angles where the closed-loop system stability analysis is highlighted. The numerical simulations have shown satisfactory results using nominal model or disturbed one compared to the use of classic sliding modes technique only. Experimental tests are performed to validate the effectiveness of the proposed control approach.

1 INTRODUCTION

Because of their layout topology, the quadrotors are capable of Vertical Take-Off and Landing (VTOL) and they have a high maneuverability. In the last couple of years, they are becoming more popular in the commercial, academic, and hobbyist sectors. The challenge that must be addressed by the researchers is to design flight controllers, insuring good performance with good level of robustness, knowing that this is a multi-variable, nonlinear and very unstable system. This has attracted the interest of many researchers in aeronautics and robotics (Yang and Lee, 2014; Bouzid et al., 2016a; Kun and Hwang, 2016).

The desire to constantly improve the performance of controlled systems leads to more complexity and may include strong nonlinearities. As the analysis and synthesis of control laws used in the linear domain are often inadequate for nonlinear systems, therefore, a little sophisticated methods then become necessary to endeavor (Zou, 2017; Bouzid et al., 2016b).

In this work, we investigate the design of an efficient control law, robust and readily implementable, which may provide good performance for VTOL vehicles in order to classify the robustness and performance level of different approaches according to operation conditions in a next forthcoming work. For this purpose, a Nonlinear PID (NLPID) control is applied to stabilize the vehicle's attitude while the tracking of 3D reference trajectories is well ensured. This controller is proposed in order to alleviate the chattering problem of the sliding mode controllers and allows a direct tuning of the controller's parameters that easily allows meeting the fixed desired specifications with good robustness level. The properties of this technique will be further discussed.

The rest of this paper is organized as follows: Section 2 introduces the mathematical model of the vehicle. Section 3 presents the synthesis of the so-called NLPID control. The application of this technique for quadrotor is described in Section 4 where a stability proof is detailed. In Section 5, the results obtained from numerical simulations as well as from the experimental tests, are given under different operating conditions. Finally, Section 6 contains the conclusion.

2 VEHICLE DYNAMICS BACKGROUND

The system operates in two coordinate frames: the inertial fixed frame $R_0(O,X,Y,Z)$ and the body

Bouzid, Y., Siguerdidjane, H. and Bestaoui, Y.
Sliding Modes based Nonlinear PID Controller for Quadrotor - Theory and Experiment.
DOI: 10.5220/0006433402860294
In *Proceedings of the 14th International Conference on Informatics in Control, Automation and Robotics (ICINCO 2017) - Volume 1*, pages 286-294
ISBN: 978-989-758-263-9

frame $R_1(O_1, X_1, Y_1, Z_1)$ (Figure 1). Let $\eta = (\varphi, \theta, \Psi)^T$ describes the orientation of the aerial vehicle (Roll, Pitch, Yaw) and $\chi = (x, y, z)^T$ denotes its absolute position with $\varphi \neq \pm\frac{\pi}{2}, \theta \neq \pm\frac{\pi}{2}$.

We give a brief explanation of the classic process followed to derive a simplified model that describes the drone's in-flight behavior where more accurate dynamic models may be found as for instance in (Kun and Hwang, 2016). The structure and the propellers are rigid and symmetric (with a suitable choice of the body reference frame as depicted in Figure 1, the inertia matrix is diagonal).

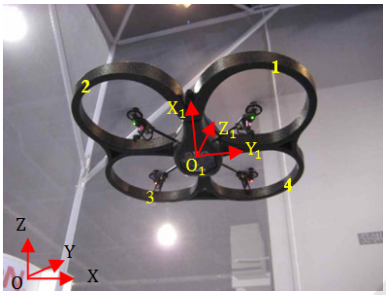

Figure 1. Quadrotor in experimentations.

Gravity force that acts on the center of mass is expressed in the earth fixed frame in the negative Z direction. The total thrust is in the positive Z direction and expressed in the body fixed frame. Then, it must be rotated into the earth fixed frame. The rotation matrix $\mathcal{R}(\varphi, \theta, \Psi)$ is given by

$$\mathcal{R} = \begin{bmatrix} c_\Psi c_\theta & c_\Psi s_\theta s_\varphi - s_\Psi c_\varphi & c_\Psi s_\theta c_\varphi + s_\Psi s_\varphi \\ s_\Psi c_\theta & s_\Psi s_\theta s_\varphi + c_\Psi c_\varphi & s_\Psi s_\theta c_\varphi - c_\Psi s_\varphi \\ -s_\theta & c_\theta s_\varphi & c_\theta c_\varphi \end{bmatrix}$$

where $s_{(.)}$ and $c_{(.)}$ are abbreviations for $sin(.)$ and $cos(.)$ respectively. Therefore, the translational dynamic may be expressed as follows

$$m\ddot{\chi} = -mge_z + u_1\mathcal{R}(\varphi, \theta, \Psi)e_z \quad (1)$$

where $e_z = (0,0,1)^T$ denotes the unit vector of Z-axis, m the mass, g the gravity acceleration and u_1 the total thrust.

Pitch and roll movements, are created by the difference in combined thrust in the opposite sides of the vehicle. However, yaw movement is generated by the differential drag forces. The rotational dynamics can be expressed as

$$I\dot{\varpi} = -\varpi \times I\varpi + G_a + \tau \quad (2)$$

$\varpi = (\varpi_x, \varpi_y, \varpi_z)^T$ denotes the angular velocity vector, $I = diag(I_x, I_y, I_z)$ is the diagonal inertia matrix, $\tau = (u_2, u_3, u_4)^T$ is the control torque and $G_a = (J_r\dot{\theta}\Omega_r, J_r\dot{\varphi}\Omega_r, 0)^T$ denotes the propellers gyroscopic effect with J_r denotes the rotors inertia and Ω_r is a mixer of the rotors speeds. The angular velocity ϖ of the quadrotor is tranformed into Euler angular speeds $\dot{\eta}$. This yields (Kun and Hwang, 2016)

$$\dot{\eta} = \begin{bmatrix} 1 & s_\varphi \tan\theta & c_\varphi \tan\theta \\ 0 & c_\varphi & -s_\varphi \\ 0 & s_\varphi / c_\theta & c_\varphi / c_\theta \end{bmatrix} \varpi \quad (3)$$

For real life applications (inspection, coverage, etc.) or hovering and by using equations (1), (2) and (3) the simplified dynamic model of the vehicle may be written as:

$$\ddot{\chi} = \begin{pmatrix} u_1 \frac{c_\Psi s_\theta c_\varphi + s_\Psi s_\varphi}{m} \\ u_1 \frac{s_\Psi s_\theta c_\varphi - c_\Psi s_\varphi}{m} \\ -g + u_1 \frac{c_\theta c_\varphi}{m} \end{pmatrix} \quad (4)$$

$$\ddot{\eta} = \begin{pmatrix} \dot{\theta}\dot{\Psi}\left(\frac{I_y - I_z}{I_x}\right) + J_r\dot{\theta}\Omega_r + \frac{u_2}{I_x} \\ \dot{\varphi}\dot{\Psi}\left(\frac{I_z - I_x}{I_y}\right) + J_r\dot{\varphi}\Omega_r + \frac{u_3}{I_y} \\ \dot{\varphi}\dot{\theta}\left(\frac{I_x - I_y}{I_z}\right) + \frac{u_4}{I_z} \end{pmatrix} \quad (5)$$

3 NONLINEAR PID CONTROLLER DESIGN

In this paper, an improvement has been brought in order to simplify the existing controllers, and thus overcome some issues poorly tackled by the classic linear or nonlinear techniques, using NLPID. Usually the kind of control called "NLPID control" stands for the regulator for which the coefficients are not assumed to be linear. More precisely, in the literature, the controllers called nonlinear PID are those with gains adjusted according to the state or those with gains depending on the phase (Seraji, 1997). Unlike those mentioned above, our control law is defined in a novel way. It consists of a nonlinear controller, which is derived from a method based upon Sliding Mode Control (SMC) theory and combined with a PID structure. In Reference (Eker, 2006), a sliding surface that has a PID structure is used in order to design a sliding mode controller. This latter is proposed to improve the performance of the standard sliding mode one. The same idea is employed later for the steering of lateral moving strip in hot strip rolling (Choi and Lee, 2009). Herein, the switching term of the sliding model is replaced by a PID structure that uses the sliding surface as an input instead of the tracking error between the reference and the measured signals.

3.1 Controller Design

Consider a class of nonlinear SISO system for $t \in [0, \infty)$ given by:

$$(\sum_x)\begin{cases}\dot{x} = \mathcal{F}(x) + G(x)u \\ y = h(x)\end{cases} \quad (6)$$

where $x \in \mathbb{R}^n$ is an n-dimentional state vector, $u \in \mathbb{R}$ is a scalar input, $y \in D_y \subset \mathbb{R}$ is a scalar output, $\mathcal{F}: D_x \dashrightarrow \mathbb{R}^n$ and $G: D_x \dashrightarrow \mathbb{R}^n$ are n-dimentional vector functions sufficiently smooth on a domain $D_x \subset \mathbb{R}^n$ and $h(x)$ the output scalar function.

Assumption (A1): *There exists a diffeomorphism $\Gamma: D_x \dashrightarrow R^n$ where $D_\xi = \Gamma(D_x)$ is a domain that contains the origin and a change of variables $\xi = \Gamma(x)$ that transforms the nonlinear system into an equivalent system given by*

$$(\sum_\xi)\begin{cases}\dot{\xi}_\iota(t) = \xi_{i+1}(t) \\ \dot{\xi}_n(t) = f(\xi) + g(\xi)u \\ y = \xi_1\end{cases} \quad (7)$$

$i = 1 \ldots n-1$. $f(\xi)$, $g(\xi)$ denote continuous nonlinear functions and $g(\xi)$ is nonsingular for all $\xi \in D_\xi$.

Now, let us consider a general sliding surface form

$$s(\varepsilon_y) = \left(\frac{d}{dt} + \lambda_y\right)^{n-1} \varepsilon_y(t) \quad (8)$$

where $\varepsilon_y = y - y_r$ represents the tracking error between a reference trajectory y_r and the output y and λ_y a positive constant.

By expansion, equation (8) may be written as

$$s(\varepsilon_y) = {\varepsilon_y}^{(n-1)}(t) + \sum_{i=0}^{n-2} \beta_i {\varepsilon_y}^{(i)}(t) \quad (9)$$

where $\beta_i, i = 0, \ldots, n-2$ are positive tuning parameters provided that they are chosen in order to render the equilibrium, $s(\varepsilon_y) = 0$, asymptotically stable in finite time T.

The first-order time derivative of $s(\varepsilon_y)$ is

$$\dot{s}(\varepsilon_y) = {\varepsilon_y}^{(n)}(t) + \sum_{i=0}^{n-2} \beta_i {\varepsilon_y}^{(i+1)} \quad (10)$$

Using the last component of system (7), where ***Assumption (A1)*** holds, equation (10) becomes

$$\dot{s}(\varepsilon_y) = f(\xi) + g(\xi)u - y_r^{(n)}(t) + \sum_{i=0}^{n-2} \beta_i {\varepsilon_y}^{(i+1)} \quad (11)$$

Given a positive definite Lyapunov function candidate

$$V = \frac{1}{2} s^2(\varepsilon_y) \quad (12)$$

The first-order time derivative of V leads to

$$\dot{V} = s(\varepsilon_y)\dot{s}(\varepsilon_y) \quad (13)$$

Note that the reachability condition of sliding mode control ensures the asymptotic stability ($\dot{V} < 0$). Thus, $\dot{s}(\varepsilon_y)$ is forced to satisfy the following inequalities

$$\begin{cases}\dot{s}(\varepsilon_y) < 0 \; when \; s(\varepsilon_y) > 0 \\ \dot{s}(\varepsilon_y) > 0 \; when \; s(\varepsilon_y) < 0\end{cases} \quad (14)$$

Assuming that

$$\dot{s}(\varepsilon_y) = -\kappa\gamma(s) \quad (15)$$

with κ being a strictly positive constant and $\gamma(s)$ is a function defined by

$$\begin{cases}\gamma(s) < 0 \; if \; s < 0 \\ \gamma(s) = 0 \; if \; s = 0 \\ \gamma(s) > 0 \; if \; s > 0\end{cases} \quad (16)$$

we ensure inequalities (14). In fact, $\gamma(s)$ may take different forms of sigmoid. The discontinuous function $\gamma(s) = sign(s)$, represents the ideal sliding modes regime.

From (11) and (15), it immediately follows that

$$u = \frac{-1}{g(\xi)}\{\kappa\gamma(s) + \sum_{i=0}^{n-2} \beta_i {\varepsilon_y}^{(i+1)} - y_r^{(n)}(t) + f(\xi)\} \quad (17)$$

The discontinuous term $\gamma(s)$ allows a good level of robustness with respect to uncertainties and disturbances. However, the fast oscillation of the control signal (chattering phenomena), gives rise of vibration in the system during the flight where these dynamics are not sustained by the rotors. So, in order to improve the performance of the controller limiting the effect of the chattering phenomena, involved through the term $\dot{s}(\varepsilon_y)$, and meet readily the specification of the control, we combine a PID structure and controller (17) determined above.

$$u = \frac{-1}{g(\xi)}\{PID + \sum_{i=0}^{n-2} \beta_i {\varepsilon_y}^{(i+1)} - y_r^{(n)}(t) + f(\xi)\} \quad (18)$$

When the state trajectory lies on the sliding surface i.e., $s(t)$= 0, the design problem of the sliding surfaces can be regarded as a linear state feedback equivalent control design. Therefore, from (17) and (18), the equivalent control is found by recognizing that $s(t)$= 0. This is a necessary condition for the state trajectory to lie on the sliding surface. As known, the switching term holds when the trajectories are not on the sliding surface in order to bring these trajectories to this surface. Therefore, we proceed by using this surface as an input of the PID structure to ensure that $s(t)$ converges toward the origin ($s(t) \to 0$) and then we ensure the convergence of the trajectories toward this surface. Therefore, the controller may be written as

$$u = \frac{-1}{g(\xi)}\left\{\begin{matrix} K_p\left(s(t) + \frac{1}{T_i}\int_0^t s(\tau)d\tau + T_d\frac{ds(t)}{dt}\right) \\ + \sum_{i=0}^{n-2} \beta_i {\varepsilon_y}^{(i+1)} - y_r^{(n)}(t) + f(\xi)\end{matrix}\right\} \quad (19)$$

K_p, T_d and T_i denote the proportional gain, the derivative and integral time constants respectively.

This new approach is clarified by Figure 2.

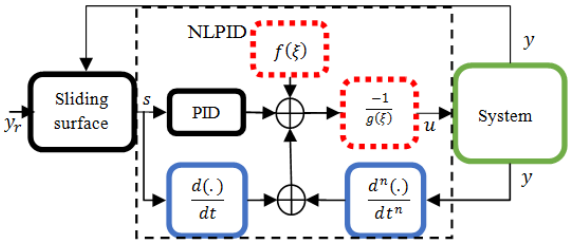

Figure 2: Nonlinear PID control architecture.

3.2 Some Properties of the Proposed Controller

The proposed technique builds on the SMC paradigm and uses a dynamic inversion-like control strategy to linearize the system. Unlike the SMC strategy, obtained controller (19) guarantees that the tracking error of the closed loop nominal linearized system goes to the origin by forcing the tracking of the sliding surface (namely $s(\varepsilon_y) = 0$) via the PID controller. The absence of actual sliding action in the proposed technique requires a proper stability theorem (see Section 4.2).

NLPID exhibits several benefits, and can be split up into two parts: The first part is involved as dynamic inversion technique in order to compensate the nonlinearities of the system. This part is represented by red colored blocks in Figure 2. The remaining part includes the PID structure, which represents the additional control needed to guarantee that the tracking error goes toward the origin by forcing the tracking of the sliding surface. We can observe in Figure 2 that sliding surface (9) is the input of the PID block instead of the tracking error as the classic one. Of course, this structure is suggested to keep almost a good level of robustness even with the absence of the discontinious term that ensures higher level of robustness.

We observe the absence of discontinuities associated to jumps in the control action, which clearly eliminates the chattering problem and reduces the consumed energy. In addition, the steady state errors are cancelled by adding the integral action that penalizes the deviations between the output and its set point. Therefore, the control accuracy is improved. Furthermore, this proposed controller allows meeting quite readily the desired specification by adjusting the PID parameters on the hovering conditions. However, the derivative term of the proposed controller induces a higher order derivative one with respect to that needed for classical "Feedback Linearization". Unfortunately, this is a drawback because of the additional noise and derivative estimation inaccuracy. These properties are shown in Section 5 through a series of numerical simulations.

4 QUADROTOR APPLICATION

This novel technique is herein applied to the quadrotor (Multi-input Multi-output system) by taking care of having an adequate control structure. In the position control, x and y are controlled through two virtual inputs (u_x, u_y) that push the system to reach the prescribed references x_r and y_r respectively and allow to generate the reference angles (φ_r, θ_r) via equation (23). The Euler angles η are controlled by the torque vector $(u_2, u_3, u_4)^T$, whereas the altitude is controlled by u_1. This control structure allows the vehicle to ensure the tracking of prescribed trajectories along the three axes (X, Y and Z) and the yaw angle. We calculate these control laws by using the NLPID approach as described in Section 3 where the tracking errors are defined as: $\varepsilon_x = x - x_r$, $\varepsilon_y = y - y_r$, $\varepsilon_z = z - z_r$, $\varepsilon_\varphi = \varphi - \varphi_r$, $\varepsilon_\theta = \theta - \theta_r$ and $\varepsilon_\Psi = \Psi - \Psi_r$.

4.1 Autopilot Design

Translation dynamics (4) can be divided into three other sub-systems along the three axis (X, Y, Z). Each sub-system has one input $(u_x, u_y, u_1$ and one output (x, y, z) respectively. We first start with u_1 for the altitude motion. Once this command is calculated we then proceed in the same way with u_x and u_y by considering u_1 as time varying parameter, with

$$\begin{cases} u_x = c_\Psi s_\theta c_\varphi + s_\Psi s_\varphi \\ u_y = s_\Psi s_\theta c_\varphi - c_\Psi s_\varphi \end{cases} \quad (20)$$

Thus, the sliding surfaces are set to:

$$s_i = \dot{\varepsilon}_i + \beta_{0i}\varepsilon_i|_{i=x,y,z} \quad (21)$$

where β_{0x}, β_{0y} and β_{0z} are positive constants.

Applying (19), we obtain

$$\begin{cases} u_1 = \frac{-m}{c_\theta c_\varphi}\left\{K_{pz}\left(s_z(t) + \frac{1}{T_{iz}}\int_0^t s_z(\tau).d\tau + T_{dz}\frac{ds_z(t)}{dt}\right) + \beta_{0z}\dot{\varepsilon}_z - g - \ddot{z}_r\right\} \\ u_x = \frac{-m}{u_1}\left\{K_{px}\left(s_x(t) + \frac{1}{T_{ix}}\int_0^t s_x(\tau).d\tau + T_{dx}\frac{ds_x(t)}{dt}\right) + \beta_{0x}\dot{\varepsilon}_x - \ddot{x}_r\right\} \\ u_y = \frac{-m}{u_1}\left\{K_{py}\left(s_y(t) + \frac{1}{T_{iy}}\int_0^t s_y(\tau).d\tau + T_{dy}\frac{ds_y(t)}{dt}\right) + \beta_{0y}\dot{\varepsilon}_y - \ddot{y}_r\right\} \end{cases} \quad (22)$$

Then, from system (20), the required reference angles of the roll and pitch rotations are given by

$$\begin{cases} \varphi_r = arcsin\left(u_x sin\,\Psi_r - u_y cos\Psi_r\right) \\ \theta_r = arcsin\left(\dfrac{u_x cos\,\Psi_r + u_y sin\Psi_r}{cos\,\varphi}\right) \end{cases} \quad (23)$$

Similarly, system (5) can be divided into three sub-systems for the roll, pitch and yaw rotations. Each one of them has one input (u_2, u_3, u_4) and one output (φ, θ, Ψ) respectively. Consequently, the surfaces are

$$\begin{cases} s_\varphi = \dot{\varepsilon_\varphi} + \beta_{0\varphi}\varepsilon_\varphi \\ s_\theta = \dot{\varepsilon_\theta} + \beta_{0\theta}\varepsilon_\theta \\ s_\Psi = \dot{\varepsilon_\Psi} + \beta_{0\Psi}\varepsilon_\Psi \end{cases} \quad (24)$$

where $(\beta_{0\varphi}, \beta_{0\theta}, \beta_{0\Psi})$ are positive constants. Finally, the control laws are given by

$$\begin{cases} u_2 = -I_x \left\{ \begin{matrix} K_{p\varphi}\left(s_\varphi(t) + \frac{1}{T_{i\varphi}}\int_0^t s_\varphi(\tau).d\tau + T_{d\varphi}\frac{ds_\varphi(t)}{dt}\right) \\ +\beta_{0\varphi}\dot{\varepsilon_\varphi} + J_r\dot{\theta}\Omega_r + \dot{\theta}\dot{\Psi}\left(\frac{I_y - I_z}{I_x}\right) - \ddot{\varphi_r} \end{matrix} \right\} \\ u_3 = -I_y \left\{ \begin{matrix} K_{p\theta}\left(s_\theta(t) + \frac{1}{T_{i\theta}}\int_0^t s_\theta(\tau).d\tau + T_{d\theta}\frac{ds_\theta(t)}{dt}\right) \\ +\beta_{0\theta}\dot{\varepsilon_\theta} + J_r\dot{\varphi}\Omega_r + \dot{\varphi}\dot{\Psi}\left(\frac{I_z - I_x}{I_y}\right) - \ddot{\theta_r} \end{matrix} \right\} \\ u_4 = -I_z \left\{ \begin{matrix} K_{p\Psi}\left(s_\Psi(t) + \frac{1}{T_{i\Psi}}\int_0^t s_\Psi(\tau).d\tau + T_{d\Psi}\frac{ds_\Psi(t)}{dt}\right) \\ +\beta_{0\Psi}\dot{\varepsilon_\Psi} + \dot{\varphi}\dot{\theta}\left(\frac{I_x - I_y}{I_z}\right) - \ddot{\Psi_r} \end{matrix} \right\} \end{cases} \quad (25)$$

Also $K_{p(.)}, T_{i(.)}, T_{d(.)}$ denote the proportional gain, the integral and derivative time constants of the NLPID structure respectively.

4.2 Stability Analysis

For the sake of completeness, we study the stability of the closed loop system using our proposed approach.

Remark 1: *all the sub-systems that describe the drone's behavior in flight (three translations and three rotations), may be considered as two-dimensional class of systems:*

For $t \in [0, \infty)$

$$\begin{cases} \dot{x}_1 = x_2 \\ \dot{x}_2 = f(\chi, \eta) + g(\chi, \eta)u \\ y = x_1 \end{cases} \quad (26)$$

where $(x_1, x_2)^T \in D_x \subset \mathbb{R}^2$ *is a 2-dimentional state vector,* $u \in \mathbb{R}$ *is a scalar input,* $y \in \mathbb{R}$ *is a scalar output.*

For $n = 2$, substituting surface expression (9) into control law (19), the closed loop of system (26) written in terms of the tracking error vector components, $\epsilon_y = \left(\varepsilon_{y_1}, \varepsilon_{y_2}\right)^T = (y - y_r, \dot{y} - \dot{y}_r)^T$ is

$$\begin{cases} \dot{\varepsilon_{y_1}} = \varepsilon_{y_2} \\ \dot{\varepsilon_{y_2}} = -\gamma_0\varepsilon_{y_1} - \gamma_1\varepsilon_{y_2} + \delta(\epsilon_y, t) \end{cases} \quad (27)$$

where:

$$\gamma_0 = \frac{K_p + T_d K_p \beta_0 + \beta_0}{1 + T_d K_p}$$

$$\gamma_1 = \frac{T_i K_p \beta_0 + K_p}{T_i(1 + T_d K_p)}$$

$$\delta(\epsilon_y, t) = \frac{K_p \beta_0}{T_i(1 + T_d K_p)} \int_0^t \varepsilon_{y_1}(\tau) d\tau$$

Consider that system (27) can be divided into nominal system

$$\dot{\epsilon_y} = \vartheta(\epsilon_y) \quad (28)$$

and an additional integral term, $\Delta(\epsilon_y, t) \in D_{\epsilon_y} \times [0, \infty) \subset \mathbb{R}^3 \dashrightarrow \mathbb{R}^2$, which equals to

$$\Delta(\epsilon_y, t) = \begin{bmatrix} 0 \\ \delta(\epsilon_y, t) \end{bmatrix}$$

Thus

$$\dot{\epsilon_y} = \vartheta(\epsilon_y) + \Delta(\epsilon_y, t) \quad (29)$$

where $\vartheta: D_{\epsilon_y} \dashrightarrow \mathbb{R}^2$ is a 2-dimentional vector functions sufficiently smooth on a domain $D_{\epsilon_y} \subset \mathbb{R}^2$.

Assuming that the origin of the nominal system is exponentially stable equilibrium and accepting that we have established this stability as following: Let V a Lyapunov function that satisfies:

$$\sigma_1\|\epsilon_y\|^2 \le V \le \sigma_2\|\epsilon_y\|^2 \quad (30)$$

The first-order time derivative along (28) is

$$\dot{V} \le -\sigma_3\|\epsilon_y\|^2 \quad (31)$$

and

$$\|\nabla V\| \le \sigma_4\|\epsilon_y\| \quad (32)$$

for all $\epsilon_y \in D_{\epsilon_y}$ and $\sigma_i > 0,\ i = 1, \dots, 4$ where ∇ denotes the gradient operator.

We suppose that $\Delta(\epsilon_y, t)$, in a bounded neighborhood of the origin, satisfies the following condition

$$\|\Delta(\epsilon_y, t)\| \le \sigma_5\|\epsilon_y\| \quad (33)$$

for all $(t, \epsilon_y) \in [0, \infty) \times D_{\epsilon_y}$ *and* $\sigma_5 > 0$.

Now, let us use V as a candidate Lyapunov function to prove the exponential stability of overall system (29). The first-order time derivative of V along (29) gives

$$\dot{V} = \nabla V^T \vartheta(\epsilon_y) + \nabla V^T \Delta(\epsilon_y, t) \quad (34)$$

Using (31), we get

$$\dot{V} \le -\sigma_3\|\epsilon_y\|^2 + \|\nabla V\|\,\|\Delta(\epsilon_y, t)\|$$

Inequalities (32) and (33) lead to

$$\dot{V} \le -\sigma_3\|\epsilon_y\|^2 + \sigma_4\sigma_5\|\epsilon_y\|^2 \quad (35)$$

To ensure that the origin of (29) is exponentially stable equilibrium, the following condition must be satisfied

$$\sigma_5 \leq \frac{\sigma_3}{\sigma_4} \tag{36}$$

We summarize this result by ***Theorem 1.***

Theorem 1: *Assuming that the origin of system* (28) *is exponentially stable. Let a Lyapunov function,* $V: D_{\epsilon_y} \dashrightarrow \mathbb{R}^+$, *defined for system* (28) *where* (30)-(32) *hold in domain* D_{ϵ_y}. *Assuming that the integral term* $\Delta(\epsilon_y, t)$ *satisfies inequality* (33), *if condition* (36) *is satisfied, then the origin of system* (29) *is also exponentially stable.*

This result is only qualitative because the above proof is done without explicit knowledge of the Lyapunov function. In the following, we seek to find a candidate Lyapunov function and the adequate parameters, σ_i, $i = 1, \dots, 5$, which verify equations (30)-(32). We propose a quadratic candidate function as

$$V(\epsilon_y) = \frac{1}{2}\epsilon_y{}^T P \epsilon_y \tag{37}$$

where

$$P = \begin{bmatrix} a_1 & a_2 \\ a_2 & a_3 \end{bmatrix}$$

is a symmetric positive definite matrix. The first-order time derivative along (28) gives

$$\begin{aligned} \dot{V}(x) = &-\gamma_0 a_2 \varepsilon_{y_1}^2 + (a_2 - \gamma_1 a_3)\varepsilon_{y_2}{}^2 \\ &+(a_1 - \gamma_1 a_2 - \gamma_0 a_3)\varepsilon_{y_1}\varepsilon_{y_2} \end{aligned} \tag{38}$$

Chosen $\sigma_3 = 1$ (see inequality (31)), equation (38) leads to:

$$\begin{cases} a_1 = \frac{\gamma_1}{\gamma_0} + \left(\frac{\gamma_0+1}{\gamma_1}\right) \\ a_2 = \frac{1}{\gamma_0} \\ a_3 = \left(\frac{\gamma_0+1}{\gamma_0\gamma_1}\right) \end{cases} \tag{39}$$

Obviously, the obtained matrix P has two eigenvalues:

$$\lambda_{1,2} = \frac{1}{2}\left(\frac{\gamma_0^2+\gamma_1^2+\gamma_0}{\gamma_0\gamma_1} + \frac{\gamma_0+1}{\gamma_0\gamma_1}\right) \mp \frac{1}{2}\sqrt{\mathcal{D}} \tag{40}$$

where

$$\begin{aligned} \mathcal{D} = &\left(\frac{\gamma_0^2+\gamma_1^2+\gamma_0}{\gamma_0\gamma_1} + \frac{\gamma_0+1}{\gamma_0\gamma_1}\right)^2 \\ &-4\left(-\frac{1}{\gamma_0^2} + \frac{\gamma_0^2+\gamma_1^2+\gamma_0}{\gamma_0\gamma_1}\left(\frac{\gamma_0+1}{\gamma_0\gamma_1}\right)\right) \end{aligned}$$

We have also

$$\nabla V = P\epsilon_y$$

Then, computing $\|\nabla V\|$ we obtain

$$\|\nabla V\| \leq \|P\|\|\epsilon_y\| \leq \sqrt{2}.eig(P)_{max}\|\epsilon_y\|$$

where $eig(P)_{max}$ is the maximal value of eigenvalues λ_1 and λ_2 of matrix P. From (32), it comes that $\sigma_4 = \sqrt{2}.eig(P)_{max}$. Then, closed loop system (29) is exponentially stable if

$$\sigma_5 \leq 1/\sqrt{2}.eig(P)_{max}$$

Theorem 2: *Let a quadratic Lyapunov function* (37), *for nominal system* (28) *on domain* D_{ϵ_y}, *where* P *is given by* (39). *If the* $\Delta(\epsilon_y, t)$ *of* (29) *satisfies inequality* (33) *with* $\sigma_5 \leq 1/\sqrt{2}.eig(P)_{max}$, *then the origin of system* (29) *is exponentially stable.*

5 SIMULATION STEP AND EXPERIMENTAL RESULTS

5.1 Numerical Simulations

Numerical simulations have been performed with the available UAV nominal parameters (Table 1).

Table 1: Quadrotor parameters.

$\boldsymbol{m(kg)}$	0.429	$\boldsymbol{I_y(kg.m^2)}$	**0.0029**
$\boldsymbol{I_X\ (kg.m^2)}$	0.0022	$I_z\ (kg.m^2)$	0.0048

The proposed controller performance is being compared with the sliding mode controller. For this purpose, we consider a vertical flight at altitude of one meter during 50 seconds. The control parameters are tuned by minimizing the following objective function using Genetic Algorithms (GA):

$$O_f = \frac{1}{t_1 - t_0}\int_{t_0}^{t_1}(\varepsilon^T\varepsilon + u^T u\ (\tau))\ d\tau$$

This is in order to obtain a good trade-off between the faster time response and the consumed energy where t_1 and t_0 are the final and the initial times respectively, $\varepsilon(\tau)$ is the tracking errors vector and u is the inputs vector. The obtained control parameters for vertical flight are: $K_{pz} = 4.289, T_{iz} = 18.527, T_{dz} = 0.001$ and $\beta_{0z} = 0.126$ for NLPID controller; $\kappa_z = 21.19$ and $\beta_{0z} = 5.18$ for SMC.

The resulting behaviors are depicted in Figure 3.

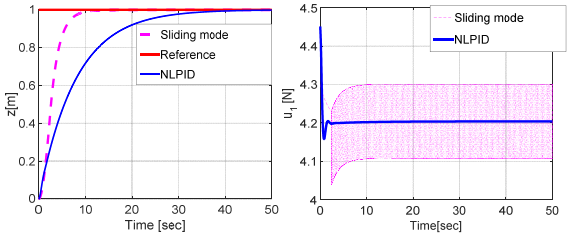

Figure 3: Comparison in vertical flight.

From Figure 3, we observe that the NLPID has a slower time response. However, the command signal is obviously improved and presents the best control behavior, which is smoothly varying without chattering. This kind of control signals is more adequate for the actuators and allows performing a

good control without vibration and with less energy. Note also that the nonlinear PID exhibits no overshoot. This is very important benefit because the overshoot of any time response creates oscillations of the vehicle during the passage from waypoint to another one. Moreover, the proposed controller achieves minor steady state error. This is due to the inclusion of an integral action term. The additional parameters are depicted in Table 2.

Table 2: Control parameters comparison.

Control parameters			
Vertical motion	Longitudinal motion	Lateral motion	Yaw rotation
NLPID			
$K_{pz} = 4.29$ $T_{iz} = 18.6$ $T_{dz} = 0.01$ $\beta_{0z} = 0.12$	$K_{px} = 4.72$ $T_{ix} = 12.43$ $T_{dx} = 0.97$ $\beta_{0x} = 9.42$ $K_{p\theta} = 0.63$ $T_{i\theta} = 1.073$ $T_{d\theta} = 0.043$ $\beta_{0\theta} = 0.56$	$K_{py} = 4.29$ $T_{iy} = 9.90$ $T_{dy} = 0.9$ $\beta_{0y} = 10.3$ $K_{p\varphi} = 0.51$ $T_{i\varphi} = 0.04$ $T_{d\varphi} = 0.70$ $\beta_{0\varphi} = 0.53$	$K_{p\Psi} = 10.8$ $T_{i\Psi} = 11.4$ $T_{d\Psi} = 0.9$ $\beta_{0\Psi} = 13.9$
SMC			
$\kappa_z = 21.19$ $\beta_{0z} = 5.18$	$\kappa_x = 29.50$ $\beta_{0x} = 5.18$ $\kappa_\theta = 1.38$ $\beta_{0\theta} = 5.26$	$\kappa_y = 30.92$ $\beta_{0y} = 6.03$ $\kappa_\varphi = 0.22$ $\beta_{0\varphi} = 4.05$	$\kappa_\Psi = 31.6$ $\beta_{0\Psi} = 5.1$

Now, let us check the effectiveness of the control laws and their level of robustness. Firstly, we consider uncertainties of 25%, 50% and 100% in the parameters with respect to the nominal values given in Table 1. Then, we suppose an additive Gaussian noise affecting the measured signals with different magnitudes of 5%, 0.5% and 0.05% respectively. The obtained results are shown in Figure 4 and Figure 5.

It should be noted from Figure 4 that the quadrotor motors generate an additional thrust at the start up in order to ensure the desired control. Furthermore, in this case of model parameters uncertainties, the controller is able to, accurately; ensure the tracking of the desired set point. Figure 5 illustrates that the high noise magnitude reduces the

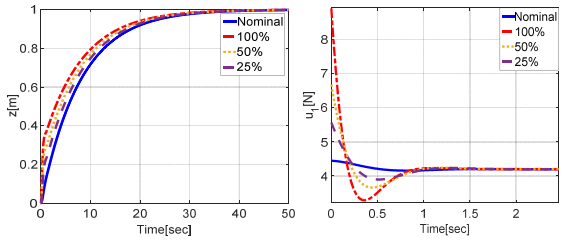

Figure 4: Comparison for parameters uncertainties scenario.

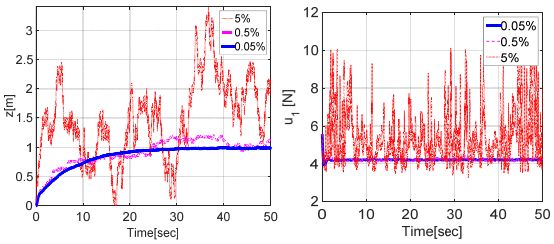

Figure 5: Comparison considering noisy measurements.

performance of the controller only, which still ensures the stability of the system.

The advantage of this novel controller is: its low sensitivity to the model uncertainties while adequate control signals are delivered.

Now, let's check the effectiveness of the controller in the case of time varying reference trajectory. For this particular example, the UAV has to stabilize its attitude while following a helix trajectory, having radius of 10 meters. The simulation-compared results are sketched in Figure 6.

Figure 6 shows the stable tracking behavior of the complete closed loop system where the outputs converge to the desired trajectory with minor steady state errors.

5.2 Experimental Results

To validate the proposed autopilot through a series of experimental tests, we have used an available X-shaped quadrotor aerial platform (AR-drone V2). The designed autopilot was implemented in C++ under Robot Operating System (ROS) open source framework using a publisher/subscriber paradigm that ensures all communications between real robots (for more details see: ros.org). The position in the plan XY is determined using the frontal camera based on Parallel Tracking and Mapping (PTAM) algorithm developed in (Engel et al., 2012). The main program runs on the ground station, which communicate with the quadrotor via Wi-Fi link.

In this simple proposed scenario, the desired trajectory is formed by successive straight-line segments. The vehicle starts from the origin to reach the point $(x, y, z) = (2m, 2m, 1m)$.

In Figure 7, we observe that the outputs converge to the desired trajectory with significant steady state accuracy. The control signals seem to be in acceptable form where the magnitudes stay within the allowable ranges (see Figure 8). Overall, this experimental test confirms the simulation results and shows the effectiveness of the technique.

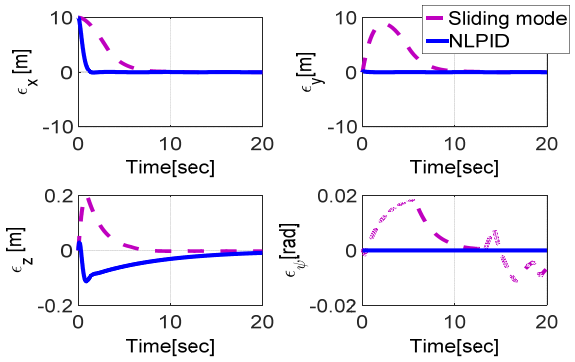

Figure 6: Tracking errors time responses.

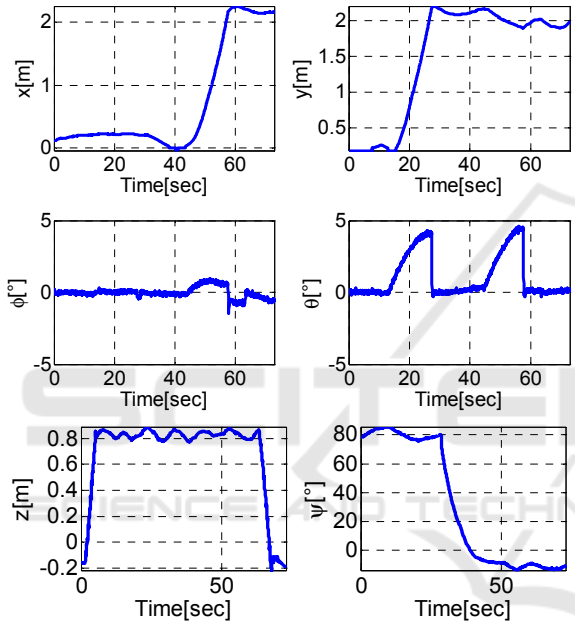

Figure 7: System time responses.

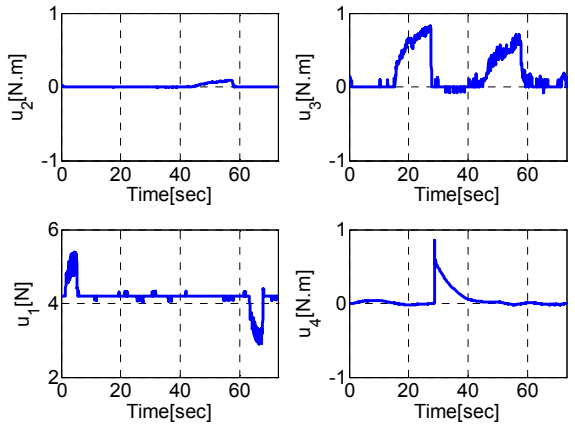

Figure 8: Control signals.

6 CONCLUSIONS

A quadrotor model was simplified in order to elaborate simple control laws for a purpose of implementation. A novel control design was proposed. It is shown that this method guarantees exponential stability. Numerical simulations were carried out in order to evaluate the effectiveness of the designed control system. Besides, experimental tests were performed. One may guess that, as matter of fact, the proposed methodology turns out to take profit of the advantages that may be brought by the PID and SMC controllers simultaneously and left aside their eventual drawbacks. In addition, the robustness against model uncertainties by choosing appropriate control parameters are guaranteed. Due to the fact that the use of sign function in the sliding mode control leads to high oscillations in the control signals, which is undesired chattering phenomenon, so, we introduced a nonstandard PID structure as a possible solution to overcome this drawback whilst the steady state errors vanishes under the effect of the integral action. In the near future work, we will study the stability of the system considering saturation modules to imitate the real case.

REFERENCES

Bouzid, Y., Siguerdidjane, H., Bestaoui, Y., Zareb, M., 2016a. Energy Based 3D Autopilot for VTOL UAV Under Guidance & Navigation Constraints. J. Intell. Robot. Syst. 1–22. doi: 10.1007/s10846-016-0441-1.

Bouzid, Y., Siguerdidjane, H., Bestaoui, Y., 2016b. Improved 3D trajectory tracking by Nonlinear Internal Model-Feedback linearization control strategy for autonomous systems. IFAC-Pap., 6th IFAC Symposium on System Structure and Control SSSC 2016Istanbul, Turkey, 22—24 June 2016 49, 13–18. doi:10.1016/j.ifacol.2016.07.480.

Choi, Y.-J., Lee, M.C., 2009. PID sliding mode control for steering of lateral moving strip in hot strip rolling. Int. J. Control Autom. Syst. 7, 399–407. doi:10.1007/s12555-009-0309-2.

Eker, İ., 2006. Sliding mode control with PID sliding surface and experimental application to an electromechanical plant. ISA Trans. 45, 109–118. doi:10.1016/S0019-0578(07)60070-6.

Engel, J., Sturm, J., Cremers, D., 2012. Accurate Figure Flying with a Quadrocopter Using Onboard Visual and Inertial Sensing, in: In Proc. of the Workshop on Visual Control of Mobile Robots (ViCoMoR) at the IEEE/RJS International Conference on Intelligent Robot Systems (IROS).

Kun, D.W., Hwang, I., 2016. Linear Matrix Inequality-Based Nonlinear Adaptive Robust Control of

Quadrotor. J. Guid. Control Dyn. 39, 996–1008. doi:10.2514/1.G001439.

Seraji, H., 1997. A New Class of Nonlinear PID Controllers for Robotic Applications.

Yang, H., Lee, D., 2014. Dynamics and control of quadrotor with robotic manipulator, in: 2014 IEEE International Conference on Robotics and Automation (ICRA). Presented at the 2014 IEEE International Conference on Robotics and Automation (ICRA), pp. 5544–5549. doi:10.1109/ICRA.2014.6907674.

Zou, Y., 2017. Nonlinear robust adaptive hierarchical sliding mode control approach for quadrotors. Int. J. Robust Nonlinear Control 27, 925–941. doi:10.1002/rnc.3607.